https://doi.org/10.5194/egusphere-2025-3763
Preprint. Discussion started: 25 August 2025

Spatiotemporal heterogeneity in diazotrophic communities reveals novel niche zonation in the East China Sea

Guangming Mai, Han Zhang, Meng Chen, Tuo Shi

Marine Genomics and Biotechnology Program, Institute of Marine Science and Technology, Shandong University, Qingdao, Shandong, PR China

Correspondence to: Tuo Shi (tuoshi@sdu.edu.cn)

Abstract. The East China Sea (ECS) is a hotspot for studying nitrogen fixation in the marginal seas of the western Pacific, where this microbially mediated process is profoundly influenced by both the coastal and oceanic current systems. Yet, how physical forcing controls the biogeography of diazotrophs and regional nitrogen budget in the ECS remains poorly characterized. Here, we carried out a cross-season survey and demonstrated dynamics in diazotrophic communities that is tightly linked to distinct water masses in the ECS. An overall spatial heterogeneity among some of the major diazotrophic ecotypes was unveiled, with the filamentous cyanobacteria *Trichodesmium* and diatom-diazotroph symbioses (Het-1 and Het-2) dominating the upper 30 m of the warm, saline, N-limited offshore water intruded by the Kuroshio and Taiwan warm current, whereas the unicellular cyanobacterial diazotrophs (UCYN-A, UCYN-B and UCYN-C) and the non-cyanobacterial diazotroph (γ-24774A11) extending their distribution further down to 60 m of the Kuroshio surface and subsurface waters. The diazotrophic abundances and nitrogen fixation rates were generally higher in autumn than in spring, suggesting a seasonal variability primarily regulated by hydrographic conditions (mainly temperature and salinity) associated with water mass movement. Modeling the distribution of diazotrophs in the water masses identified five taxon-specific niches occupied by eight distinct diazotrophic ecotypes. Taken together, our analyses provide mechanistic insights into the role of dominant forms of physical forcing in driving the spatiotemporal variability in diazotrophic distribution and activity in the ECS, which is of important reference in assessing diazotrophs adaptation in a changing marine ecosystem.

https://doi.org/10.5194/egusphere-2025-3763
Preprint. Discussion started: 25 August 2025

Introduction

Nitrogen is an essential nutrient for sustaining life on Earth. Although nitrogen is abundant in the atmosphere as dinitrogen gas (N_2), it is largely unusable in this form to most organisms on the planet. For nitrogen to be able to make biomolecules such as proteins, nucleic acids, and chlorophyll, it must first be converted into biologically available ammonia (NH_3) through N_2 fixation, a process mediated by a select group of prokaryotes termed diazotrophs (Zehr and Capone, 2020). This biologically fixed nitrogen fuels primary production and carbon export in the ocean, thus ultimately affecting global carbon and nitrogen cycles (Falkowski, 1997; Karl et al., 1997; Wang et al., 2019). While much research has been devoted to N_2 fixation in the open ocean (e.g., Chen et al., 2019; Shao et al., 2023; Wen et al., 2022), accumulating evidence suggests the potential of coastal aquatic system as a significant yet underappreciated source of global N budget (Fulweiler et al., 2025; Tang et al., 2019). As the vital ecotones bridging terrestrial and marine ecosystems, coastal waters exhibit pronounced environmental gradients shaped by land-ocean interactions. These complex conditions challenge our understanding of the physicochemical processes involved in regulating the distribution and activity of marine diazotrophs (Fontela et al., 2025; Jiang et al., 2023a, b; Tang et al., 2019). Delineating the dynamics of diazotrophic biogeography in the nearshore environment is, therefore, key to modeling regional nitrogen cycle and resolving disparate accounts of fixed nitrogen budget globally (Fulweiler et al., 2025; Tang et al., 2019; Tang and Cassar, 2019; Zehr and Capone, 2020).

The East China Sea (ECS) is a temperate marginal sea in the western North Pacific with complex hydrodynamic conditions governed by the East Asian monsoon as well as the intrusion of Kuroshio, a vigorous western boundary current as it enters the ECS off the northeast Taiwan (Fig. 1; Cui et al., 2021; Qiu and Imasato, 1990). The intruded Kuroshio is typically divided into two layers, the Kuroshio surface water (KSW, upper 120 m) and the Kuroshio subsurface water (KSSW, 120–250 m) (Chen et al., 1995). At approximately 27.5°N/122°E, the KSSW bifurcates into the offshore and nearshore Kuroshio branch currents, with the latter transporting rich nutrients into the shelf region, particularly in summer (Yang et al., 2012, 2018). Meanwhile, Taiwan warm current (TWC), a mixture of waters from the Taiwan Strait and the Kuroshio, flows northward on the ECS shelf and occasionally reaches the Changjiang Estuary (Zhou et al., 2015). It has been shown that the southwest monsoon can enhance the transport of Kuroshio and TWC during

https://doi.org/10.5194/egusphere-2025-3763
Preprint. Discussion started: 25 August 2025

warm seasons (Yang et al., 2018; Zhou et al., 2015), whereas the inshore ECS region is strongly influenced by the Changjiang diluted water (CDW) and the coastal water (CW), both of which are notably expanded seaward under the influence of the northeast monsoon (Yue et al., 2021). Thus, the dynamic interplay between these water masses creates steep biogeochemical gradients across the ECS shelf (Chen, 2009; Zhang et al., 2007). The upwelling of nutrient-rich KSSW, coupled with terrestrial inputs from CDW and CW, may fuel phytoplankton growth in the coastal regions (e.g., Gao et al., 2025; Sun et al., 2025). In contrast, the warm, saline, and nutrient-poor KSW and TWC establish favorable habitats for diazotroph communities and N_2 fixation (Jiang et al., 2018, 2019, 2023a, b). Previous studies have demonstrated that changes in hydrographic conditions can control nutrient fluxes and planktonic community shifts throughout the ECS ecosystem (Jiang et al., 2018, 2019, 2023a, b; Sun et al., 2025), however, the detailed patterns of diazotrophs distribution in the ECS in relation to different water masses remain poorly characterized.

Recent studies have elucidated Kuroshio intrusion as a key driver in transporting filamentous cyanobacterial diazotrophs, including the free-living *Trichodesmium* and the diatom-associated symbionts (Jiang et al., 2018, 2019, 2023a, b), to the Changjiang Estuary during warm seasons, significantly elevating the rates of N_2 fixation in the Kuroshio waters expanding toward the shelf region compared to the CDW and CW (Jiang et al., 2023a, b). The distribution of unicellular diazotrophs in relation to water mass-driven hydrographic processes in the ECS, however, has not been adequately examined. Given the dominance of unicellular diazotrophs and their potential contributions to N_2 fixation in Kuroshio (Cheung et al., 2017, 2019; Lee Chen et al., 2014; Wu et al., 2018), and a currently disproportionate research focus on the filamentous *Trichodesmium* populations in individual seasons (Jiang et al., 2017, 2019, 2023a, b; Yue et al., 2021), systematic investigation into the compositional dynamics of unicellular diazotrophs in the ECS is urgently needed. Furthermore, water mass movements in the ECS are seasonally modulated by the East Asian monsoon (Yin et al., 2018), and the seasonal variability in current patterns is projected to be strengthened in climate models (Vélez-Belchí et al., 2013; Yang et al., 2024), thus necessitating a comprehensive understanding of how increasingly intensified water mass movements may restructure the distribution of distinct diazotrophic ecotypes in the ECS (Tang and Cassar, 2019).

Realized niche modeling provides a trait-based framework for analysing biogeographic patterns by

https://doi.org/10.5194/egusphere-2025-3763
Preprint. Discussion started: 25 August 2025

examining species fitness and their ecological responses to environmental changes (Edwards et al., 2013; Irwin et al., 2012; Litchman et al., 2012), which has been integrated into biogeochemical models to predict species distribution under future climate change scenarios (Irwin et al., 2012, 2015). Maximum entropy method, a species distribution model for characterizing the realized niche, has proven particularly effective for quantifying species-environment relationships from sparse field observations (Irwin et al., 2012; Phillips et al., 2006). Consistent patterns in phytoplankton realized niches across geographical regions (Brun et al., 2015; Irwin et al., 2012) have been depicted using long-term observational datasets from the western Pacific marginal seas (Xiao et al., 2018; Zhong et al., 2020), the North Atlantic (Irwin et al., 2012, 2015), and the global open ocean (Brun et al., 2015), showing that functionally analogous taxa (e.g., coccolithophores) occupy more similar niches than taxonomically distinct groups (e.g., diatoms). Despite the progress in modeling phytoplankton ecology in general, our understanding of realized niches of diazotrophic communities remains fragmented (Brun et al., 2015). This knowledge gap fundamentally limits our ability to predict N_2 fixation in the global ocean in response to climate change, especially in the highly variable temperate marginal seas.

To illuminate the patterns and drivers of N_2 fixation in the ECS, we conducted a cross-season survey analyzing the distribution, abundance and activity of the major diazotrophic ecotypes known to date, alongside hydrographic analysis and integrated niche modeling approaches. Our analyses reveal spatiotemporal heterogeneity in diazotrophic distribution and N_2 fixation rate, which is highly correlated with distinct water masses. Overall, the realized niche partitioning presented here emphasizes the role of physical forcing (e.g., Kuroshio intrusion) in shaping the diversity and biogeography of diazotrophs in a marginal sea with complex land-ocean interactions.

2 Materials and methods

2.1 Field sampling and environmental parameter collection

We conducted a cross-season survey at 42 stations in the ECS aboard the research vessel *Xiang Yang Hong 18* during the 2023 summer (October 13–30) and 2024 spring (April 9–24) (Fig. 1). At each station, temperature and salinity were acquired from a Seabird 911plus conductivity–temperature–depth sampler

https://doi.org/10.5194/egusphere-2025-3763
Preprint. Discussion started: 25 August 2025

(Sea-Bird Electronics, USA) and binned over 1 m depth intervals. For biological and environmental sample collection, seawater was collected at 3 or 7 discrete depths throughout the upper 100 m using Niskin bottles. Approximately 2 L of seawater was prefiltered through a 200 μm pore-size nylon mesh to remove large zooplankton, followed by filtration onto a 0.2 μm pore-size PES membrane filter (Pall, USA). The membranes were flash-frozen in liquid N_2 for subsequent DNA extraction. Seawater samples for nutrient analyses were filtered through 0.2 μm pore-size polycarbonate membranes (Millipore, USA) and then dispensed into 100 mL acid-washed polyethylene bottles and stored at –20°C. Nitrate plus nitrite (hereafter abbreviated as NO_x) and soluble reactive phosphorus (SRP) concentrations were analyzed using a Technicon AA3 AutoAnalyzer (Bran Luebbe, Germany). The N:P ratios were calculated based on the molar ratio of NO_x and SRP, and the excess SRP (P^*) was determined as $P^* = SRP – NO_x/16$ (Anderson and Sarmiento, 1994). Water samples for chlorophyll *a* (Chl *a*) measurement were collected on GF/F membranes (Whatman, USA), incubated in 90% acetone (v/v) overnight at 4°C and measured using a Trilogy fluorometer (Turner Designs, USA). Seawater samples for RNA analysis were collected at 7 stations (Fig. 5) in the upper 50 m using acid-rinsed Nalgene polycarbonate bottles during the day (13:00–15:30 local time) or at night (21:40–3:40 local time) to mirror diel variations in nitrogenase reductase gene (*nifH*) expression (Church et al., 2005; Moisander et al., 2014). Each sample was taken by filtering 4.5 L of seawater onto a 0.2 μm pore-size PES membrane (Pall, USA), which was soaked in 1 mL of RNAlater (ThermoFisher, USA) and then instantly refrigerated in liquid N_2 for later extraction. Surface seawater was also obtained from 21 stations of the study area to measure the rates of N_2 fixation (Fig. 6), with details described below.

2.2 DNA and RNA extraction

DNA was extracted using the cetyltrimethylammonium bromide method as described by Zhang et al. (2024). The concentration and purity of DNA were determined using a NanoPhotometer N50 spectrophotometer (Implen, Germany). RNA was extracted with TRI Regent (Molecular Research Center, USA), and the extracted RNA was subjected to DNA digestion and purification using a Direct-zol RNA Miniprep kit (Zymo, USA). DNA contamination in purified RNA was checked by amplifying the bacterial 16S rRNA gene with universal primers 341F and 806R (Wasimuddin et al., 2020). The *nifH* mRNA was reversely transcribed to synthesize complementary DNA (cDNA) using a RevertAid RT kit (Thermo Fisher Scientific, USA) with

https://doi.org/10.5194/egusphere-2025-3763
Preprint. Discussion started: 25 August 2025

the gene-specific reverse transcription (RT)-primers *nifH*2 and *nifH*3 (Moisander et al., 2014), following the manufacturer's protocol.

2.3 TaqMan qPCR assay of targeted *nifH* genes and transcripts

TaqMan quantitative PCR (qPCR) was performed to quantify *nifH* gene and transcript abundances of the nine major diazotrophic phylotypes, including *Trichodesmium*, diatom-diazotroph symbioses (Het-1, Het-2 and Het-3), the unicellular cyanobacterial diazotrophs (UCYN-A1, UCYN-A2, UCYN-B and UCYN-C) and the non-cyanobacterial diazotroph (γ-24774A11), using established primer and probe sets (Table S1; Church et al., 2005a, b; Foster et al., 2007; Langlois et al., 2008; Moisander et al., 2008, 2010; Thompson et al., 2014). The reference *nifH* sequences used for making standard curves were synthesized at Sangon Biotech (Shanghai, China; Table S1). Duplicate qPCR assays were run for each DNA/cDNA sample and the standards on a CFX96 real-time system (Bio-Rad Laboratories, USA). Each reaction mixture (10 μL) contained 5 μL of Premix Ex Taq (Takara Bio, Japan), 0.4 μM each of the forward and reverse primers, 0.4 μM of TaqMan probe, 2 μL of template DNA or cDNA, and nuclease-free water (Thermo Fisher Scientific). The thermal cycling conditions were 50°C for 2 min, 95°C for 2 min, and 45 cycles of 95°C for 15 s, followed by 60°C (64°C for UCYN-A2) for 1 min. A standard curve was generated by serial dilutions of a known concentration of the *nifH* references, and the negative controls were also included in each run to check contamination. Although UYN-A2 is currently considered an early-stage N_2-fixing organelle ("nitroplast") (Coale et al., 2024), we have maintained its designation as a N_2-fixing organism throughout our study to simplify the comparison with conventional diazotrophs. Considering that this qPCR assay could amplify UCYN-A2 together with relatively high abundances of UCYN-A3 and UCYN-A4 (Cheung et al., 2017, 2019; Farnelid et al., 2016), we referred to the target collectively as UCYNA2/A3/A4.

2.4 Measurement of nitrogen fixation rate

Nitrogen fixation rates (NFRs) were determined using the $^{15}N_2$ gas dissolution method (Mohr et al., 2010; Großkopf et al., 2012; Montoya et al., 1996). Briefly, 0.22 μm-filtered seawater was degassed using a Sterapore membrane unit (20M1500A; Mitsubishi Rayon, Japan) and then stored in a Tedlar bag without headspaces (Shiozaki et al., 2015). After that, the $^{15}N_2$ gas stock (99%; Cambridge Isotope Laboratories, USA)

https://doi.org/10.5194/egusphere-2025-3763
Preprint. Discussion started: 25 August 2025

was injected into the bag at a ratio of 10 mL of $^{15}N_2$ gas per 1 L of seawater. The bag was gently tapped until the gas was fully equilibrated. At designated stations, duplicate acid-cleaned 2.3-L polycarbonate bottles were filled with bubble-free surface seawater, each spiked with 200 mL of $^{15}N_2$-enriched seawater and then incubated on deck for 24 h. Incubated samples were filtered (vacuum pressure <200 mm Hg) onto pre-combusted (450°C, 4 h) GF75 membranes (Advantec, Japan), which were immediately stored in liquid N_2 until onshore processing for particulate organic N (PON) and ^{15}N abundance measurements. Unamended natural seawater samples were also collected for comparison as a blank control. The PON and ^{15}N abundances were analyzed using an elemental analyzer interfaced with an isotope ratio mass spectrometry (Thermo Fisher Scientific). The NFR was calculated according to Montoya et al. (1996), and the minimum quantifiable NFR for each station ranged from 0.12 to 0.74 nmol N L^{-1} d^{-1} (Gradoville et al., 2017).

2.5 Statistical analyses

To identify the hydrographic dynamics induced by distinct water masses, an optimum multiparameter analysis (OMP; Tomczak and Large, 1989) was applied to calculate their contribution at each sampling depth. The method quantitatively evaluates the mixing ratios of source water types (SWTs) based on quasi-conservative properties (e.g., temperature and salinity) by solving a series of linear equations. Based on previous studies (Chen, 2009; Yang et al., 2012) and the temperature-salinity diagram (Fig. S1), the ECS is primarily influenced by the CDW/CW, TWC, KSW and KSSW, and we determined the properties (temperature and salinity) of CDW/CW by the observational data from stations SF1 (31.16°N/122.56°E) and SF2 (30.49°N/122.67°E), and the properties of other SWTs (i.e., TWC, KSW and KSSW) by the modeled data from the World Ocean Atlas 2023 dataset (Table S2; Locarnini et al., 2024; Reagan et al., 2024). The OMP was carried out with Python package “pyompa” (Shrikumar et al., 2022).

To determine the mean (μ) and breadth (σ) of diazotrophic realized niches in relation to environmental variables, we integrated published data (Cheung et al., 2019; Sato et al., 2024; Shiozaki et al., 2018) with field observations in the ECS in a combined framework implementing the Maximum entropy method (MaxEnt; Phillips et al., 2006) and generalized additive model (GAM), as described by Xiao et al. (2018). Principal component analysis (PCA) was utilized to discern the relationships between diazotrophic phylotypes and the realized niches. Ward’s minimum variance clustering was conducted based on Euclidean

https://doi.org/10.5194/egusphere-2025-3763
Preprint. Discussion started: 25 August 2025

distances calculated from standardized scores of the first two PCA components. The optimal cluster number was determined by analyzing within-cluster sum of squared errors through an elbow plot across candidate cluster numbers.

A Wilcoxon signed-rank test was employed to assess the significant differences (p<0.05) in biological and environmental variables across regions and sampling seasons because of the violation of assumptions related to normality and homogeneity of variance. Redundancy analysis (RDA) was adopted to detect the effects of environmental factors associated with distinct water masses (z-score scaling) on diazotrophic phylotypes (Log_{10} transformation). The P^* and KSSW variables were excluded from the RDA due to collinearity in the models. The RDA, PCA and clustering analysis were performed with R (version 4.1.3, http://www.r-project.org, last access: 10 March 2025) package "vegan" (Oksanen et al., 2024), GAM with R package "mgcv" (Wood, 2011), and pie chart with R package "scatterpie" (Yu, 2025).

3 Results

3.1 Environmental conditions

The physicochemical parameters in the ECS showed apparent spatial variations during autumn and spring (Fig. 2). Sea surface temperature was significantly higher in autumn (23.1–27.6°C) than that in spring (14.0–25.8°C; p<0.05) (Fig. 2A and F), while no significant seasonal difference was detected in salinity, though autumn values had lower range (29.7–34.4 PSU) compared to spring (26.6–34.6 PSU) (Fig. 2B and G). Horizontally, the highest temperature (>25°C) and salinity (>34 PSU) were observed on the outer ECS shelf, accompanied by high proportions (>80%) of KSW and TWC (Fig. S2B, C, F and G), indicating strong intrusions from these water masses. In contrast, the lowest temperature and salinity values were found mainly in the coastal regions influenced by CDW/CW (>60% in proportion; Fig. S2A and E). Particularly in spring, the seaward extension of CDW/CW (temperature <18°C and salinity <31 PSU) was strongly enhanced under the East Asian monsoon (Fig. S2E). Vertically, the cold (<20°C), saline (>34 PSU) waters dominated the bottom layer along the transects A and B during the sampling seasons (Fig. S3), indicating significant KSSW intrusions (>80% in proportion) on the ECS shelf (Fig. S2D and H). Surface NO_x concentration in autumn (0.44–17.71 μM) was in a narrower range than that in spring (0.16–19.11 μM), but the values were 6–12

https://doi.org/10.5194/egusphere-2025-3763
Preprint. Discussion started: 25 August 2025

times higher in nearshore waters relative to offshore regions in both seasons (p<0.05; Fig. 2C and H). However, SRP content was found to be comparable between these regions during autumn (0.14–0.91 μM; Fig. 2D) and spring (0.14–0.84 μM; Fig. 2I), suggesting that CDW/CW and KSW may be important sources for SRP in nearshore and offshore environments, respectively. The N:P ratio exhibited a lower range in autumn (1.3–19.5) compared to spring (0.4–37.3), but exceeded the Redfield ratio (16) in coastal waters in both seasons, mirroring the spatial distribution pattern of NO_x (Fig. 2E and J).

3.2 Variations in the distribution of major planktonic diazotrophs

Significant spatial heterogeneity in *nifH* gene abundance between autumn and spring was observed in almost all the diazotrophic phylotypes examined except Het-3, which remained undetectable in qPCR assay (Fig. 3). In autumn, *Trichodesmium* emerged as the dominant diazotroph, reaching up to 6.6×10^5 copies L^{-1} at surface and 9.2×10^9 copies m^{-2} throughout the water column (Fig. 3A and C). *Trichodesmium* accounted for approximately 90% of the *nifH* gene pools in the ECS, with both the surface and depth-integrated abundances increasing along the coast-to-offshore transects. Additionally, Hets (Het-1 and Het-2), UCYN-B and γ-24774A11 were found primarily in the southeastern ECS, with 1–2 orders of magnitude lower in abundance than *Trichodesmium*. The abundances of the UCYN-A (UCYN-A1 and UCYN-A2/A3/A4) were mostly below 1.0×10^3 copies L^{-1} in the surveyed areas. In spring, the targeted diazotrophs were mostly undetectable, except at some of stations in the southeastern ECS, where *Trichodesmium* was the most abundant (up to 6.0×10^5 copies L^{-1} at surface and 1.1×10^{10} copies m^{-2} throughout the water column), followed by UCYN-A1 (up to 1.7×10^5 copies L^{-1} and 8.4×10^9 copies m^{-2}) (Fig. 3B and D). The abundances of the other targeted diazotrophs (Hets, UCYN-A2/A3/A4, UCYN-B, UCYN-C and γ-24774A11) varied between 1.0×10^3 and 3.0×10^4 copies L^{-1} in the ECS.

The targeted diazotrophs also exhibited seasonal variations in vertical distribution (Fig. 4 and S4). The averaged *nifH* gene abundances of *Trichodesmium* and Hets in the upper 50 m were considerably higher in autumn than those in spring, but this seasonal difference diminished gradually with increasing depths (Fig. 4A–C). Remarkably, UYCN-B displayed the seasonal abundance difference continuously throughout the water column (Fig. 4F). In contrast, the UCYN-A and UCYN-C in the upper 50 m were markedly less abundant in autumn than that in spring (Fig. 4D, E and G), while γ-24774A11 showed no depth-dependent

https://doi.org/10.5194/egusphere-2025-3763
Preprint. Discussion started: 25 August 2025

seasonal variation (Fig. 4H). Moreover, profiling along the transects A (stations 22–30) and B (stations 36–42) revealed that *Trichodesmium* was more widely distributed in autumn compared to spring, but its abundance consistently peaked (>10^5 copies L^{-1}) in the upper 30 m during both seasons (Fig. S4A–D). The Hets were also distributed mainly in the upper 30 m, and most abundant (>10^4 copies L^{-1}) in the southeastern ECS during spring (Fig. S4E–L). Compared to Het-1, Het-2 showed a broader distribution during the sampling seasons. Notably, the unicellular diazotrophs (UCYN-A, UYCN-B, UCYN-C and γ-24774A11) were most abundant at depths of 0–60 m (Fig. S4M–Z), demonstrating moderately deeper distributions relative to their filamentous counterparts (*Trichodesmium* and Hets). Overall, all targeted diazotrophic groups displayed apparently reduced abundances below the 60-m layer, possibly due to low temperature imposed by KSSW intrusion (Fig. S3 and S4).

3.3 Pattern of *nifH* transcription in the targeted diazotrophs

Transcription of the *nifH* gene in the targeted diazotrophs generally mirrored the observed gene abundance pattern but displayed greater seasonal variability across the stations (Fig. 5). In autumn, the *nifH* transcripts of *Trichodesmium* were the most abundant among 6 of the 7 stations sampled, ranging from 6.8×10^3 to 1.7×10^5 *nifH* transcripts L^{-1} at surface and from 5.1×10^4 to 2.4×10^6 *nifH* transcripts m^{-2} in the upper 50 m (Fig. 5A and C). The *nifH* transcripts of Het-2 and UCYN-B were similarly high in the southeastern ECS (8.0×10^3 *nifH* transcripts L^{-1} at surface and 1.7×10^5 *nifH* transcripts m^{-2} in the upper 50-m water column). The *nifH* transcripts of Het-1 and γ-24774A11 were 1–2 orders of magnitude lower relative to the other targeted diazotrophs. Overall, *Trichodesmium* dominated the *nifH* transcript pool (>70%) of the targeted diazotrophs, except at station 30 where Het-2 (40%) and UCYN-B (40%) exhibited relatively higher abundance. In spring, the *nifH* transcripts were only detected at 2 of the 7 stations sampled (Fig. 5B and D). At station 30, *Trichodesmium*, Het-1, UYN-A1 and UCYN-B equally dominated the *nifH* transcript pools at surface and in the upper 50-m water column. At station 40, however, *Trichodesmium*, Het-1 and UYN-A1 transcripts were abundant at surface, whereas UCYN-B prevailed at depths of 10–50 m. Despite the station-to-station variations, some diazotrophs exhibited distinct diel variations in *nifH* transcription (Fig. S5). The *nifH* transcription levels of *Trichodesmium*, Het-1 and UYCN-A were significantly higher at daytime (Fig. S5A, B, D and E), whereas Het-2 and UYCN-B mainly expressed the *nifH* gene at night (Fig. S5C and F).

https://doi.org/10.5194/egusphere-2025-3763
Preprint. Discussion started: 25 August 2025

The γ-24774A11 displayed no detectable diel pattern in *nifH* transcription (Fig. S5G).

3.4 Seasonal variations in the rates of nitrogen fixation

The NFRs in surface waters exhibited distinct seasonal variations in the ECS (Fig. 6). In autumn, the NFRs ranged from undetectable to 6.22 nmol N L^{-1} d^{-1} (1.39 ± 2.14 nmol N L^{-1} d^{-1} on average). The rates were higher at Kuroshio-influenced stations (e.g., 20 and 30), but lower in the CDW/CW-affected regions (e.g., stations 1, 31, and 37). In spring, the NFRs ranged from undetectable to 1.77 nmol N L^{-1} d^{-1} (0.84 ± 0.16 nmol N L^{-1} d^{-1} on average) and were only half of the autumn rates on average. The NFRs were also relatively low in the CDW/CW-affected regions.

3.5 Correlation between diazotroph abundances and environmental variables in distinct water masses

In both seasons, the diazotrophic abundances were positively correlated with temperature and salinity, but negatively correlated with water depth, nutrient concentration, and N:P ratio (Fig. 7). This pattern indicates that the distribution of these diazotrophs was primarily constrained by the KSW, with characteristic high temperature and salinity, shallow water depth, and oligotrophic conditions. Furthermore, Chl *a* exerted limited influence on the targeted diazotrophic groups except for Het-2, which showed positive correlation with Chl *a* concentration in spring (Fig. 7B).

We characterized the realized niche mean (μ) and breadth (σ) of the diazotrophs in the ECS with combined hydrographic, environmental and biological data (Fig. S6), and identified five distinct clusters among the diazotrophs (Fig. 8 and S7). *Trichodesmium* exhibited lower, broader temperature and salinity niches ($\mu_{Temperature}$ = 23.3°C, $\sigma_{Temperature}$ = 8.9°C, $\mu_{Salinity}$ = 33.2 PSU and $\sigma_{Salinity}$ = 1.4 PSU) as well as higher nutrient niches (μ_{NOx} = 7.70 μM, μ_{SRP} = 0.55 μM and $\mu_{N:P}$ = 6.56). In contrast, UCYN-A1 and UCYN-A2/A3/A4 clustered together and dominated in high-salinity habitats (34.4 PSU), demonstrating significant ecological overlap among the UCYN-A. Nonetheless, significant differences in niche distribution existed between UCYN-B and UCYN-A, with the former inhabiting relatively nutrient-rich niches (μ_{NOx} = 4.23 μM and μ_{SRP} = 0.47 μM). Additionally, the Hets and UCYN-C clustered together, and were characterized by high mean temperature (25.0°C) and P^* (0.51 μM) niches. The γ-24774A11 was abundant in habitats between UCYN-A and Hets, and its temperature and salinity niches were relatively high as well.

https://doi.org/10.5194/egusphere-2025-3763
Preprint. Discussion started: 25 August 2025

4 Discussion

4.1 Spatial distribution of key planktonic diazotrophs in the ECS

Temperature and nutrient availability are widely recognized as key environmental factors governing the biogeographical distribution and physiological constraints of filamentous diazotrophs (Chen et al., 2019; Tang and Cassar, 2019; Tuo et al., 2021). As expected, our quantification of the *nifH* gene copies showed that *Trichodesmium* and Hets were more abundant on the warm, saline, and N-limited outer ECS shelf (Fig. 3), which was constantly intruded by the Kuroshio and TWC (Fig. S2B, C, F and G). In contrast, the cold, fresh, and N-rich CDW/CW (Fig. S2A and E) restricted the growth and abundance of these two phylotypes in coastal waters. The pattern of *Trichodesmium* and Hets distribution in the ECS was consistent with earlier microscopy-based observations (Jiang et al., 2018, 2019, 2023a, b), and positively correlated with temperature and salinity but negatively with nutrient concentrations (Fig. 7). Additionally, our result revealed the presence of unicellular diazotrophs (UCYN-A, UCYN-B, UCYN-C and γ-24774A11; $>5\times10^4$ *nifH* gene copies L^{-1}) in Kuroshio-influenced waters, but complete absence in the CDW/CW-dominated regions (Fig. 3 and S2). Highly abundant UCYN-A1, UCYN-B and γ-24774A11 ($>10^4$ *nifH* gene copies L^{-1}) were consistently found in Kuroshio, particularly in its upstream region (Chen et al., 2019; Wen et al., 2022) and surface waters spanning from northeastern Taiwan to south coast of mainland Japan (Cheung et al., 2019; Shiozaki et al., 2018). It is, therefore, reasonable to attribute the prevalence of unicellular diazotrophs on the outer ECS shelf to the lateral transport by Kuroshio mainstream, as proved by the positive correlation between their abundance and Kuroshio intrusion (Fig. 7). Overall, filamentous diazotrophs (mainly *Trichodesmium*) represented approximately 70% of the total *nifH* genes across most of the surveyed areas, confirming them as primary N_2 fixers in the ECS (Jiang et al., 2023a, b). On the other hand, unicellular diazotrophs, particularly UCYN-A1 and UCYN-B, occasionally dominated in the Kuroshio-influenced regions, suggesting their potential contribution to regional N_2 fixation (Lee Chen et al., 2014; Wu et al., 2018). Arguably, given the lack of observed *Trichodesmium* colonies in our samples, the prefiltration through a 200-μm pore-size nylon mesh did not underestimate its abundance.

Despite a gradual decrease in abundance with increasing depths, the diazotrophs exhibited taxon-specific vertical distributions in the ECS (Fig. 4 and S4). Specifically, the filamentous diazotrophs

https://doi.org/10.5194/egusphere-2025-3763
Preprint. Discussion started: 25 August 2025

(*Trichodesmium* and Hets) showed maximum abundance in the upper 30 m (Fig. S4A–L), contrasting with earlier reports of subsurface maxima (30–50 m) in the ECS (Jiang et al., 2018, 2019) and other regions (Carpenter et al., 2004; Liu et al., 2023). The discrepancy among these studies may be due to the variations in both available nutrients (e.g., SRP and iron) and light intensities (Turk-Kubo et al., 2018; Wen et al., 2022) on the site of the ongoing surveys (Fig. 2D and I). Additionally, the lack of anticyclonic eddies during our sampling time is likely to eliminate the downward entrainment of *Trichodesmium* in deeper water column (Jiang et al., 2018). In contrast, the unicellular diazotrophs (UCYN-A, UCYN-B, UCYN-C and γ-24774A11) were distributed mainly in the upper 60 m, extending moderately deeper than their filamentous counterparts (Fig. S4). A similar pattern was also observed in the northern South China Sea (SCS; Lu et al., 2019) and western North/South Pacific (Stenegren et al., 2018; Wen et al., 2022). Compared with the filamentous diazotrophs, the lower light saturation coefficients of the unicellular cyanobacterial diazotrophs (Garcia et al., 2013; Gradoville et al., 2021; Shen et al., 2024) may enable them to dominate in dim, deep waters (Lu et al., 2018). Moreover, the KSSW intrusion-induced low temperature (~20.5°C) environment at depths of 30–60 m may also account for the dominance of the unicellular diazotrophs (Fig. S3 and S4), whose optimal growth temperature (~22°C for UCYN-A2 and UCYN-B) (Mak et al., 2025; Shao and Luo, 2022; Webb et al., 2009) is substantially lower than that of the filamentous ecotypes (~26°C for *Trichodesmium* and Hets) (Breitbarth et al., 2007; Fu et al., 2014; Tang and Cassar, 2019). Unfortunately, while the lifestyle of photoheterotrophic metabolism (Langlois et al., 2015; Moisander et al., 2014) has been proposed, how γ-24774A11 thrives in the euphotic zone remains uncharacterized (Shao and Luo, 2022). Resolving the metabolic strategies of γ-24774A11 is hence critical for elucidating its ecological niche and modeling its biogeochemical contributions in marine ecosystem (Cornejo-Castillo and Zehr, 2021).

4.2 Seasonal variations in diazotrophic distribution and nitrogen fixation rates in the ECS

In addition to the spatial heterogeneity, our results also revealed pronounced seasonal dynamics in diazotrophic distribution in the ECS (Figs. 3 and S4), primarily driven by the synergistic interplay between monsoonal hydrographic forcing and diazotrophic taxon-specific characteristics. In autumn, the southwest monsoon intensified the northward and shoreward penetration of Kuroshio and TWC onto the ECS shelf (>80%; Fig. S2B and C), establishing warm (>24°C), NO_x-deplete (<1 μM) water mass (Fig. 2 and S2) that

https://doi.org/10.5194/egusphere-2025-3763
Preprint. Discussion started: 25 August 2025

favored the proliferation of *Trichodesmium* (Fig. 3A and C), while increasing the coastal shoaling of CDW/CW. The dominance of *Trichodesmium* in the ECS is likely attributed to the *r*-selected life history strategy (Koening et al., 2009), which enables it to outcompete other diazotrophs when nutrients (e.g., SRP and iron) become available (Chen et al., 2019; Tyrrell, 2003). This pattern is consistent with the extensive observations in Kuroshio-affected, island-adjacent waters where *Trichodesmium* dominates the diazotrophic community (Lee Chen et al., 2003; Shiozaki et al., 2015). In spring, however, the northeast monsoon facilitated the offshore expansion of the CDW/CW, resulting in decreased *Trichodesmium* abundance in the cold (<20°C), NO_x-replete (>1 μM) northern ECS, but increased abundance in the warm, NO_x-deplete southern ECS (Fig. 3B and D). Regarding the unicellular diazotrophs, UCYN-A and UCYN-C were 4–5 orders of magnitude more abundance in spring than in autumn, but the seasonal variation was not significant for UCYN-B (Fig. 3 and S4M–V). The distribution of UCYN-A and UCYN-C was positively correlated to higher salinity in spring (>34.5 PSU; Fig. 7B and S3), a pattern also observed in previous studies (Li et al., 2021; Shiozaki et al., 2018), but the underlying mechanism is unknown.

Our data also showed seasonal dynamics in N_2 fixation in the ECS, with higher NFRs in autumn relative to spring, particularly in Kuroshio-affected waters dominated by *Trichodesmium* (i.e., stations 5, 20 and 30; Fig. 3 and 6). The averaged autumn NFR was similar to what has been reported during summer in the ECS (Jiang et al., 2023a), despite the differences in NFR measurement between the two studies (i.e., dissolution versus bubble methods). The decreased NFRs in spring may be related to a substantial decrease in abundance and activity of *Trichodesmium* (Fig. 3A and B), which has been suggested to account for approximately 60% of the bulk NFRs on the outer ECS shelf (Jiang et al., 2023a, b). On the other hand, the low temperature (14–20 °C) in spring could otherwise promote the prevalence of non-cyanobacterial diazotrophs and their contribution to N_2 fixation, particularly in CDW/CW-affected waters (Jiang et al., 2023b), but this pattern was not observed in our dataset (Fig. 3 and 6). Notably, the seasonal dynamics of NFRs were not significantly correlated with transcriptional abundances of diazotrophs (Fig. 5 and 6), suggesting that the expression of *nifH* gene in diazotrophs may not be synchronized with actual nitrogenase activity (Turk-Kubo et al., 2012).

To assess the contribution of key diazotrophs to the N budget, we extrapolated NFRs in the water column by applying published, cell-specific rates of N_2 fixation in *Trichodesmium*, Hets, UCYN-A, and UCYN-B

https://doi.org/10.5194/egusphere-2025-3763
Preprint. Discussion started: 25 August 2025

(Table S3). We based our depth-integrated assessment on two assumptions: 1) NFRs were considered constant throughout the water column, neglecting the regulation by environmental variables such as light, temperature and nutrient availability (e.g., Lu et al., 2018; Jiang et al., 2023a, b); 2) One *nifH* gene copy per cell was used for computational simplification, despite the environmentally and/or phylogenetically driven variations in the cellular *nifH* gene copies (Gradoville et al., 2022; Sargent et al., 2016; Shao et al., 2023). Given the depth-integrated abundance of the targeted diazotrophs, the averaged NFRs in the ECS ranged from 58.5 μmol N m^{-2} d^{-1} in spring to 238.0 μmol N m^{-2} d^{-1} in autumn (Table S3). The huge seasonal disparity may result from the absence of cyanobacterial diazotrophs at most of the sampling stations in spring (Fig. 3). Nevertheless, the estimated NFRs in the high-salinity waters remained consistently high during autumn (333.4 μmol N m^{-2} d^{-1}) and spring (343.8 μmol N m^{-2} d^{-1}; Fig. 3; Table S3), approximating those determined in the southeastern ECS (Jiang et al., 2023a). Notably, filamentous diazotrophs (mostly *Trichodesmium*) contributed 97% and 88% of the bulk NFRs in autumn and spring (Table S3), respectively, significantly exceeding those documented previously in the northern SCS and upstream Kuroshio (Lee Chen et al., 2014), and the western Pacific (Bonnet et al., 2009; Kitajima et al., 2009). However, the relative contributions of filamentous diazotrophs in the southeastern ECS during spring could be potentially overestimated as the cellular copy number of *nifH* gene in *Trichodesmium* is characteristically high (Sargent et al., 2016; Shao et al., 2023), which may complicate the quantitative assessments here. Moreover, failure to incorporate non-cyanobacterial diazotrophs into the bulk NFR assessments due to lack of cell-specific data may weaken their ecological contribution to the N budget, particularly in cold environments where they sustain active N_2 fixation (Fig. 2 and 6) (Lin et al., 2013). To elucidate the distinction between filamentous and unicellular diazotrophs in their contributions to N_2 fixation in the ECS, highly-resolved NFR measurements completely spanning the four seasons and across fine scales of size-fractionated sampling should be emphasized in future studies (Jiang et al., 2023b).

4.3 Spatiotemporal dynamics in diazotrophic distribution reveals niche zonation

Our analysis revealed taxon-specific diazotrophic distribution that is closely linked to adjacent water masses (Fig. 7 and S4), identifying five distinct clusters of diazotrophic ecotypes in the multidimensional niche space in the ECS (Fig. 3 and 8). *Trichodesmium* alone formed a unique cluster with a broader tolerance to

https://doi.org/10.5194/egusphere-2025-3763
Preprint. Discussion started: 25 August 2025

temperature, salinity, and nutrients (Fig. 8 and S6) than the open-ocean population (Brun et al., 2015). The significantly expanded niche breadth of *Trichodesmium* may arise from both intraspecific metabolic plasticity (Knapp et al., 2012; Knapp, 2012; Turk-Kubo et al., 2018) and interspecific physiological differences (Carpenter et al., 1993), as the dominance of *T. erythraeum* in coastal waters and *T. thiebautii* on the ECS shelf has been demonstrated (Jiang et al., 2018; Zhang et al., 2019). These strategic adaptations underpin *Trichodesmium*'s widespread distribution in the ECS (Fig. 3). In contrast, the UCYN-A exhibited high-salinity and low-nutrient preference while maintaining broad thermal tolerance (Fig. 8 and S6), coinciding with their spring proliferation in the oligotrophic Kuroshio (Fig. 3B and D), which may be suited to the symbiosis between UCYN-A and its eukaryotic host (Gérikas Ribeiro et al., 2018; Sun et al., 2014). Different from UCYN-A, the broad temperature and nutrient niche preference of UCYN-B (Fig. 8 and S6) supported its persistence in both the warmer, saline, oligotrophic KSW and the cooler, equally saline, eutrophic KSSW (Fig. S4Q–T). The acclimation to low temperature in UCYN-B may stem from either the compensatory effects of its high-nutrient niche (Deng et al., 2022) or interspecific thermal adaptation diversity within the UCYN-B populations (Webb et al., 2007; Zehr et al., 2007). A niche differentiation was also observed between UCYN-B and *Trichodesmium* (Fig. 8), consistent with previous findings in the southern SCS (Zhang et al., 2024) and the western Pacific (Chen et al., 2019). Unlike UCYN-B, the Hets and UCYN-C exhibited higher, narrower temperature ranges coupled with elevated P^* and reduced NO_x requirements (Fig. 8 and S6), causing their distribution confined in KSW enriched with terrestrial and/or aerosol-derived SRP (Fig. 2D, I and 3). Such conditions have been shown to enhance symbiotic associations between Hets and diatom hosts (Tuo et al., 2014) and promote UCYN-C growth (Turk-Kubo et al., 2015) in tropical oceans. Moreover, the γ-24774A11 had niche traits that are intermediate between those of UCYN-A and Hets (Fig. 8 and S6), particularly the preference to high-temperature, high-salinity, and low-nutrient conditions. While these specialized traits may facilitate the cosmopolitan distribution of γ-24774A11 in sunlit surface waters, its sustained population viability under elevated NO_x concentrations is often observed in the field (Bird and Wyman, 2013; Shao and Luo, 2022; Shiozaki et al., 2014). More systematic, eco-physiological investigations are needed to resolve this apparent niche contradiction and clarify its biogeographic patterns (Cornejo-Castillo and Zehr, 2021).

https://doi.org/10.5194/egusphere-2025-3763
Preprint. Discussion started: 25 August 2025

We also observed overlap in realized niches among some of the diazotrophic groups (Fig. 8). For example, there was a partial overlap in niche distribution between Het-1 and Het-2 in the Kuroshio-dominated regions, with the latter exhibiting a broader temperature niche (Fig. 3 and S4). Moreover, UCYN-C appeared to be clustered with the Hets (Fig. 8), but the former had a much higher salinity niche (Fig. S7B). A significant positive correlation in distribution and abundance between UCYN-C and Het-1 has been reported in the western Pacific (Chen et al., 2019). It has also been suggested that *Epithemia pelagica*, a diatom-associated cyanobacterial diazotroph closely affiliated to UCYN-C, may share ecological niches with the Hets (Cheung et al., 2019; Schvarcz et al., 2022). However, due to potential cross reactivity between the *nifH* primers and probes designed in the qPCR assays (Cheung et al., 2019; Schvarcz et al., 2022), the niche overlap between UCYN-C and Hets deserves further investigations. Furthermore, we found a co-occurrence pattern between UCYN-A1 and UCYN-A2/A3/A4, which is commonly observed in the open oceans (Cabello et al., 2016; Gérikas Ribeiro et al., 2018; Nguyen et al., 2025), with the latter exhibiting lower abundance and narrower vertical distribution range (Fig. 3 and S4M–P). It seems that the distinct reproductive strategies of the UCYN-A hosts may explain the niche differences between the UCYN-A (Fig. 3 and S4M–P) (Cabello et al., 2016). The UCYN-A1 host appears to adopt an *r*-strategy favoring rapid growth under favorable conditions, while the UCYN-A2/A3/A4 host likely employs a *K*-strategy characterized by persistence at low abundances and enhanced competitiveness in stable, low-nutrient environments (Cabello et al., 2016).

Data availability

All data needed to evaluate the conclusions in the paper are present in Figs. 1–8 and/or the Supplement. Additional data associated with the paper are available from the corresponding authors upon request.

Author contributions

TS conceived and designed the study. GM participated in the expedition cruises and collected the samples. GM, HZ, and MC contributed to the reagents, materials, and analysis tools. GM and MC analyzed the data. GM, HZ, MC, and TS drafted the manuscript. All authors read and approved the final version of the manuscript.

https://doi.org/10.5194/egusphere-2025-3763
Preprint. Discussion started: 25 August 2025

Competing interests

The authors declare that they have no conflict of interest.

Acknowledgements

The authors are grateful to the captain and crew of the R/V *Xiang Yang Hong 18* for logistics at sea and help with collection of the hydrographic data. We extend our special thanks to Xianyao Zhang and Yidong Xue for assistance with sampling, Mengjiao Shi, Xiaosong Zhong and Xiangbin Ran for providing the nutrient and chlorophyll *a* data, and Wupeng Xiao for discussion with data analysis. The authors also thank the reviewers for their insightful comments that helped improve the clarity of the manuscript.

Financial support

This research has been supported by the National Natural Science Foundation of China (grant numbers 41676092, 42076152 and 32401350) and the Natural Science Foundation of Shandong Province of China (grant number ZR2023QD124). The work aligns with the mission of global ocean negative carbon emission program (https://www.global-once.org).

References

Anderson, L. A. and Sarmiento, J. L.: Redfield ratios of remineralization determined by nutrient data analysis, Glob. Biogeochem. Cycles, 8, 65–80, https://doi.org/10.1029/93gb03318, 1994.

Bird, C. and Wyman, M.: Transcriptionally active heterotrophic diazotrophs are widespread in the upper water column of the Arabian Sea, FEMS Microbiol. Ecol., 84, 189–200, https://doi.org/10.1111/1574-6941.12049, 2013.

Bonnet, S., Biegala, I. C., Dutrieux, P., Slemons, L. O., and Capone, D. G.: Nitrogen fixation in the western equatorial Pacific: Rates, diazotrophic cyanobacterial size class distribution, and biogeochemical significance, Glob. Biogeochem. Cycles, 23, 2008GB003439, https://doi.org/10.1029/2008GB003439, 2009.

Breitbarth, E., Oschlies, A., and LaRoche, J.: Physiological constraints on the global distribution of

https://doi.org/10.5194/egusphere-2025-3763
Preprint. Discussion started: 25 August 2025

Trichodesmium – effect of temperature on diazotrophy, Biogeosciences, 4, 53–61, https://doi.org/10.5194/bgd-3-779-2006, 2007.

Brun, P., Vogt, M., Payne, M. R., Gruber, N., O'Brien, C. J., Buitenhuis, E. T., Le Quéré, C., Leblanc, K., and Luo, Y.: Ecological niches of open ocean phytoplankton taxa, Limnol. Oceanogr., 60, 1020–1038, https://doi.org/10.1002/lno.10074, 2015.

Cabello, A. M., Cornejo-Castillo, F. M., Raho, N., Blasco, D., Vidal, M., Audic, S., De Vargas, C., Latasa, M., Acinas, S. G., and Massana, R.: Global distribution and vertical patterns of a prymnesiophyte–cyanobacteria obligate symbiosis, ISME J., 10, 693–706, https://doi.org/10.1038/ismej.2015.147, 2016.

Carpenter, E., O'Neil, J., Dawson, R., Siddiqui, P., Roenneberg, T., and Bergman, B.: The tropical diazotrophic phytoplankter *Trichodesmium*: biological characteristics of two common species, Mar. Ecol. Prog. Ser., 95, 295–304, https://doi.org/10.3354/meps095295, 1993.

Carpenter, E. J., Subramaniam, A., and Capone, D. G.: Biomass and primary productivity of the cyanobacterium *Trichodesmium* spp. in the tropical N Atlantic ocean, Deep-Sea Res. Pt. I, 51, 173–203, https://doi.org/10.1016/j.dsr.2003.10.006, 2004.

Chen, C. T. A., Ruo, R., Paid, S. C., Liu, C. T., and Wong, G. T. F.: Exchange of water masses between the East China Sea and the Kuroshio off northeastern Taiwan, Cont. Shelf Res., 15, 19–39, https://doi.org/10.1016/0278-4343(93)E0001-O, 1995.

Chen, C.-T. A.: Chemical and physical fronts in the Bohai, Yellow and East China seas, J. Mar. Syst., 78, 394–410, https://doi.org/10.1016/j.jmarsys.2008.11.016, 2009.

Chen, M., Lu, Y., Jiao, N., Tian, J., Kao, S., and Zhang, Y.: Biogeographic drivers of diazotrophs in the western Pacific Ocean, Limnol. Oceanogr., 64, 1403–1421, https://doi.org/10.1002/lno.11123, 2019.

Cheung, S., Suzuki, K., Saito, H., Umezawa, Y., Xia, X., and Liu, H.: Highly heterogeneous diazotroph communities in the Kuroshio current and the Tokara Strait, Japan, PLoS One, 12, e0186875, https://doi.org/10.1371/journal.pone.0186875, 2017.

Cheung, S., Suzuki, K., Xia, X., and Liu, H.: Transportation of diazotroph community from the upstream to downstream of the Kuroshio, J. Geophys. Res.-Biogeo., 124, 2680–2693, https://doi.org/10.1029/2018JG004960, 2019.

https://doi.org/10.5194/egusphere-2025-3763
Preprint. Discussion started: 25 August 2025

Church, M., Jenkins, B., Karl, D., and Zehr, J.: Vertical distributions of nitrogen-fixing phylotypes at Stn ALOHA in the oligotrophic North Pacific Ocean, Aquat. Microb. Ecol., 38, 3–14, https://doi.org/10.3354/ame038003, 2005a.

Church, M. J., Short, C. M., Jenkins, B. D., Karl, D. M., and Zehr, J. P.: Temporal patterns of nitrogenase gene (*nifH*) expression in the oligotrophic North Pacific Ocean, Appl. Environ. Microbiol., 71, 5362–5370, https://doi.org/10.1128/AEM.71.9.5362-5370.2005, 2005b.

Coale, T. H., Loconte, V., Turk-Kubo, K. A., Vanslembrouck, B., Mak, W. K. E., Cheung, S., Ekman, A., Chen, J.-H., Hagino, K., Takano, Y., Nishimura, T., Adachi, M., Le Gros, M., Larabell, C., and Zehr, J. P.: Nitrogen-fixing organelle in a marine alga, Science, 384, 217–222, https://doi.org/10.1126/science.adk1075, 2024.

Cornejo-Castillo, F. M. and Zehr, J. P.: Intriguing size distribution of the uncultured and globally widespread marine non-cyanobacterial diazotroph Gamma-A, ISME J., 15, 124–128, https://doi.org/10.1038/s41396-020-00765-1, 2021.

Cui, X., Yang, D., Sun, C., Feng, X., Gao, G., Xu, L., and Yin, B.: New insight into the onshore intrusion of the Kuroshio into the East China Sea, J. Geophys. Res.-Oceans, 126, e2020JC016248, https://doi.org/10.1029/2020JC016248, 2021.

Deng, L., Cheung, S., Kang, C., Liu, K., Xia, X., and Liu, H.: Elevated temperature relieves phosphorus limitation of marine unicellular diazotrophic cyanobacteria, Limnol. Oceanogr., 67, 122–134, https://doi.org/10.1002/lno.11980, 2022.

Edwards, K. F., Litchman, E., and Klausmeier, C. A.: Functional traits explain phytoplankton community structure and seasonal dynamics in a marine ecosystem, Ecol. Lett., 16, 56–63, https://doi.org/10.1111/ele.12012, 2013.

Falkowski, P. G.: Evolution of the nitrogen cycle and its influence on the biological sequestration of CO_2 in the ocean, Nature, 387, 272–275, https://doi.org/10.1038/387272a0, 1997.

Farnelid, H., Turk-Kubo, K., Muñoz-Marín, M., and Zehr, J.: New insights into the ecology of the globally significant uncultured nitrogen-fixing symbiont UCYN-A, Aquat. Microb. Ecol., 77, 125–138, https://doi.org/10.3354/ame01794, 2016.

https://doi.org/10.5194/egusphere-2025-3763
Preprint. Discussion started: 25 August 2025

Fontela, M., Fernández-Román, D., Broullón, E., Farnelid, H., Fernández-Carrera, A., Marañón, E., Martínez-García, S., Rodríguez-Ramos, T., Varela, M. M., and Mouriño-Carballido, B.: Puzzling out the ecological niche construction for nitrogen fixers in a coastal upwelling system, ISME Commun., 5, ycaf018, https://doi.org/10.1093/ismeco/ycaf018, 2025.

Foster, R. A., Subramaniam, A., Mahaffey, C., Carpenter, E. J., Capone, D. G., and Zehr, J. P.: Influence of the Amazon River plume on distributions of free-living and symbiotic cyanobacteria in the western tropical north Atlantic Ocean, Limnol. Oceanogr., 52, 517–532, https://doi.org/10.4319/lo.2007.52.2.0517, 2007.

Fu, F., Yu, E., Garcia, N., Gale, J., Luo, Y., Webb, E. A., and Hutchins, D. A.: Differing responses of marine N_2 fixers to warming and consequences for future diazotroph community structure, Aquat. Microb. Ecol., 72, 33–46, https://doi.org/10.3354/ame01683, 2014.

Fulweiler, R. W., Rinehart, S., Taylor, J., Kelly, M. C., Berberich, M. E., Ray, N. E., Oczkowski, A., Balint, S., Benavides, M., Church, M. J., Loeks, B., Newell, S., Olofsson, M., Oppong, J. C., Roley, S. S., Vizza, C., Wilson, S. T., Chowdhury, S., Groffman, P., Scott, J. T., and Marcarelli, A. M.: Global importance of nitrogen fixation across inland and coastal waters, Science, 388, 1205–1209, https://doi.org/10.1126/science.adt1511, 2025.

Gao, J., Bi, R., Sachs, J. P., Wang, Y., Ding, Y., Che, H., Zhang, J., Yao, P., Shi, J., and Zhao, M.: Assessing the interaction of oceanic and riverine processes on coastal phytoplankton dynamics in the East China Sea, Mar. Life Sci. Technol., 7, 157–175, https://doi.org/10.1007/s42995-024-00260-y, 2025.

Garcia, N. S., Fu, F.-X., Breene, C. L., Yu, E. K., Bernhardt, P. W., Mulholland, M. R., and Hutchins, D. A.: Combined effects of CO_2 and light on large and small isolates of the unicellular N_2-fixing cyanobacterium *Crocosphaera watsonii* from the western tropical Atlantic Ocean, Eur. J. Phycol., 48, 128–139, https://doi.org/10.1080/09670262.2013.773383, 2013.

Gérikas Ribeiro, C., Lopes Dos Santos, A., Marie, D., Pereira Brandini, F., and Vaulot, D.: Small eukaryotic phytoplankton communities in tropical waters off Brazil are dominated by symbioses between Haptophyta and nitrogen-fixing cyanobacteria, ISME J., 12, 1360–1374, https://doi.org/10.1038/s41396-018-0050-z, 2018.

https://doi.org/10.5194/egusphere-2025-3763
Preprint. Discussion started: 25 August 2025

Gradoville, M. R., Bombar, D., Crump, B. C., Letelier, R. M., Zehr, J. P., and White, A. E.: Diversity and activity of nitrogen-fixing communities across ocean basins, Limnol. Oceanogr., 62, 1895–1909, https://doi.org/10.1002/lno.10542, 2017.

Gradoville, M. R., Cabello, A. M., Wilson, S. T., Turk-Kubo, K. A., Karl, D. M., and Zehr, J. P.: Light and depth dependency of nitrogen fixation by the non-photosynthetic, symbiotic cyanobacterium UCYN-A, Environ. Microbiol., 23, 4518–4531, https://doi.org/10.1111/1462-2920.15645, 2021.

Gradoville, M. R., Dugenne, M., Hynes, A. M., Zehr, J. P., and White, A. E.: Empirical relationship between *nifH* gene abundance and diazotroph cell concentration in the North Pacific Subtropical Gyre, J. Phycol., 58, 829–833, https://doi.org/10.1111/jpy.13289, 2022.

Großkopf, T., Mohr, W., Baustian, T., Schunck, H., Gill, D., Kuypers, M. M. M., Lavik, G., Schmitz, R. A., Wallace, D. W. R., and LaRoche, J.: Doubling of marine dinitrogen-fixation rates based on direct measurements, Nature, 488, 361–364, https://doi.org/10.1038/nature11338, 2012.

Irwin, A. J., Nelles, A. M., and Finkel, Z. V.: Phytoplankton niches estimated from field data, Limnol. Oceanogr., 57, 787–797, https://doi.org/10.4319/lo.2012.57.3.0787, 2012.

Irwin, A. J., Finkel, Z. V., Müller-Karger, F. E., and Troccoli Ghinaglia, L.: Phytoplankton adapt to changing ocean environments, Proc. Natl. Acad. Sci., 112, 5762–5766, https://doi.org/10.1073/pnas.1414752112, 2015.

Jiang, Z., Chen, J., Zhou, F., Zhai, H., Zhang, D., and Yan, X.: Summer distribution patterns of *Trichodesmium* spp. in the Changjiang (Yangtze River) Estuary and adjacent East China Sea shelf, Oceanologia, 59, 248–261, https://doi.org/10.1016/j.oceano.2017.02.001, 2017.

Jiang, Z., Li, H., Zhai, H., Zhou, F., Chen, Q., Chen, J., Zhang, D., and Yan, X.: Seasonal and spatial changes in *Trichodesmium* associated with physicochemical properties in East China Sea and southern Yellow Sea, J. Geophys. Res.-Biogeo., 123, 509–530, https://doi.org/10.1002/2017JG004275, 2018.

Jiang, Z., Chen, J., Zhai, H., Zhou, F., Yan, X., Zhu, Y., Xuan, J., Shou, L., and Chen, Q.: Kuroshio shape composition and distribution of filamentous diazotrophs in the East China Sea and southern Yellow Sea, J. Geophys. Res.-Oceans, 124, 7421–7436, https://doi.org/10.1029/2019JC015413, 2019.

Jiang, Z., Zhu, Y., Sun, Z., Zhai, H., Zhou, F., Yan, X., Zeng, J., Chen, J., and Chen, Q.: Enhancement of

https://doi.org/10.5194/egusphere-2025-3763
Preprint. Discussion started: 25 August 2025

summer nitrogen fixation by the Kuroshio intrusion in the East China Sea and southern Yellow Sea, J. Geophys. Res.-Biogeo., https://doi.org/10.1029/2022JG007287, 2023a.

Jiang, Z., Zhu, Y., Sun, Z., Zhai, H., Zhou, F., Yan, X., Chen, Q., Chen, J., and Zeng, J.: Size-fractionated N_2 fixation off the Changjiang Estuary during summer, Front. Microbiol., 14, 1189410, https://doi.org/10.3389/fmicb.2023.1189410, 2023b.

Karl, D., Letelier, R., Tupas, L., Dore, J., Christian, J., and Hebel, D.: The role of nitrogen fixation in biogeochemical cycling in the subtropical North Pacific Ocean, Nature, 388, 533–538, https://doi.org/10.1038/41474, 1997.

Kitajima, S., Furuya, K., Hashihama, F., Takeda, S., and Kanda, J.: Latitudinal distribution of diazotrophs and their nitrogen fixation in the tropical and subtropical western North Pacific, Limnol. Oceanogr., 54, 537–547, https://doi.org/10.4319/lo.2009.54.2.0537, 2009.

Knapp, A., Dekaezemacker, J., Bonnet, S., Sohm, J., and Capone, D.: Sensitivity of *Trichodesmium erythraeum* and *Crocosphaera watsonii* abundance and N_2 fixation rates to varying NO_3^- and PO_4^{3-} concentrations in batch cultures, Aquat. Microb. Ecol., 66, 223–236, https://doi.org/10.3354/ame01577, 2012.

Knapp, A. N.: The sensitivity of marine N_2 fixation to dissolved inorganic nitrogen, Front. Microbiol., 3, 374, https://doi.org/10.3389/fmicb.2012.00374, 2012.

Koening, M. L., Wanderley, B. E., and Macedo, S. J.: Microphytoplankton structure from the neritic and oceanic regions of Pernambuco State – Brazil, Braz. J. Biol., 69, 1037–1046, https://doi.org/10.1590/S1519-69842009000500007, 2009.

Langlois, R., Großkopf, T., Mills, M., Takeda, S., and LaRoche, J.: Widespread distribution and expression of Gamma A (UMB), an uncultured, diazotrophic, γ-proteobacterial *nifH* phylotype, PLoS One, 10, e0128912, https://doi.org/10.1371/journal.pone.0128912, 2015.

Langlois, R. J., Hümmer, D., and LaRoche, J.: Abundances and distributions of the dominant *nifH* phylotypes in the northern Atlantic Ocean, Appl. Environ. Microbiol., 74, 1922–1931, https://doi.org/10.1128/AEM.01720-07, 2008.

Lee Chen, Y., Chen, H., and Lin, Y.: Distribution and downward flux of *Trichodesmium* in the South China

https://doi.org/10.5194/egusphere-2025-3763
Preprint. Discussion started: 25 August 2025

Sea as influenced by the transport from the Kuroshio current, Mar. Ecol. Prog. Ser., 259, 47–57, https://doi.org/10.3354/meps259047, 2003.

Lee Chen, Y., Chen, H.-Y., Lin, Y.-H., Yong, T.-C., Taniuchi, Y., and Tuo, S.: The relative contributions of unicellular and filamentous diazotrophs to N_2 fixation in the South China Sea and the upstream Kuroshio, Deep-Sea Res. Pt. I, 85, 56–71, https://doi.org/10.1016/j.dsr.2013.11.006, 2014.

Li, L., Wu, C., Huang, D., Ding, C., Wei, Y., and Sun, J.: Integrating stochastic and deterministic process in the biogeography of N_2-fixing cyanobacterium *Candidatus* Atelocyanobacterium Thalassa, Front. Microbiol., 12, 654646, https://doi.org/10.3389/fmicb.2021.654646, 2021.

Lin, F., Chen, M., Yang, W., Zhang, R., Zheng, M., Qiu, Y., Tong, J., Lin, Z., and Zhang, X.: Biological N_2 fixation in the East China Sea in spring 2009, J. Appl. Oceanogr., 32, 445–454. https://doi.org/10.3969/J.ISSN.2095-4972.2013.04.001, 2013.

Litchman, E., Edwards, K., Klausmeier, C., and Thomas, M.: Phytoplankton niches, traits and eco-evolutionary responses to global environmental change, Mar. Ecol. Prog. Ser., 470, 235–248, https://doi.org/10.3354/meps09912, 2012.

Liu, J., Zhang, H., Ding, X., Zhou, L., Ke, Z., Li, J., and Tan, Y.: Nitrogen fixation under the interaction of Kuroshio and upwelling in the northeastern South China Sea, Deep-Sea Res. Pt. I, 200, 104147, https://doi.org/10.1016/j.dsr.2023.104147, 2023.

Liu, Z., Gan, J., Hu, J., Wu, H., Cai, Z., and Deng, Y.: Progress of studies on circulation dynamics in the East China Sea: The Kuroshio exchanges with the shelf currents, Front. Mar. Sci., 8, 620910, https://doi.org/10.3389/fmars.2021.620910, 2021.

Locarnini, R. A., Mishonov, A. V., Baranova, O. K., Reagan, J. R., Boyer, T. P., Seidov, D., Wang, Z., Garcia, H. E., Bouchard, C., Cross, S. L., Paver, C. R., and Dukhovskoy, D.: World Ocean Atlas 2023, Volume 1: Temperature, https://doi.org /10.25923/54bh-1613, 2024.

Lu, Y., Wen, Z., Shi, D., Chen, M., Zhang, Y., Bonnet, S., Li, Y., Tian, J., and Kao, S.-J.: Effect of light on N_2 fixation and net nitrogen release of *Trichodesmium* in a field study, Biogeosciences, 15, 1–12, https://doi.org/10.5194/bg-15-1-2018, 2018.

Lu, Y., Wen, Z., Shi, D., Lin, W., Bonnet, S., Dai, M., and Kao, S.: Biogeography of N_2 fixation influenced

https://doi.org/10.5194/egusphere-2025-3763
Preprint. Discussion started: 25 August 2025

by the western boundary current intrusion in the South China Sea, J. Geophys. Res.-Oceans, 124, 6983–6996, https://doi.org/10.1029/2018jc014781, 2019.

Mak, E. W. K., Turk-Kubo, K. A., Voznyuk, A. V., Gradoville, M. R., Coale, T., Hagino, K., and Zehr, J. P.: Temperature-dependent growth and activity in a globally distributed nitrogen-fixing haptophyte, Limnol. Oceanogr., 70, 1499–1511, https://doi.org/10.1002/lno.70050, 2025.

Mohr, W., Großkopf, T., Wallace, D. W. R., and LaRoche, J.: Methodological underestimation of oceanic nitrogen fixation rates, PLoS One, 5, e12583, https://doi.org/10.1371/journal.pone.0012583, 2010.

Moisander, P. H., Beinart, R. A., Voss, M., and Zehr, J. P.: Diversity and abundance of diazotrophic microorganisms in the South China Sea during intermonsoon, ISME J., 2, 954–967, https://doi.org/10.1038/ismej.2008.51, 2008.

Moisander, P. H., Beinart, R. A., Hewson, I., White, A. E., Johnson, K. S., Carlson, C. A., Montoya, J. P., and Zehr, J. P.: Unicellular cyanobacterial distributions broaden the oceanic N_2 fixation domain, Science, 327, 1512–1514, https://doi.org/10.1126/science.1185468, 2010.

Moisander, P. H., Serros, T., Paerl, R. W., Beinart, R. A., and Zehr, J. P.: Gammaproteobacterial diazotrophs and *nifH* gene expression in surface waters of the South Pacific Ocean, ISME J., 8, 1962–1973, https://doi.org/10.1038/ismej.2014.49, 2014.

Montoya, J. P., Voss, M., Hler, P. K., and Capone, D. G.: A simple, high-precision, high-sensitivity tracer assay for N_2 fixation, Appl. Environ. Microbiol., 62, 986–993, https://doi.org/10.1128/aem.62.3.986-993.1996, 1996.

Nguyen, A., Ustick, L. J., Larkin, A. A., and Martiny, A. C.: Global phylogeography and microdiversity of the marine diazotrophic cyanobacteria *Trichodesmium* and UCYN-A, mSphere, 10, e00245-25, https://doi.org/10.1128/msphere.00245-25, 2025.

Oksanen, J., Simpson, G. L., Blanchet, F. G., Kindt, R., Legendre, P., Minchin, P. R., O'Hara, R. B., Solymos, P., Stevens, M. H. H., Szoecs, E., Wagner, H., Barbour, M., Bedward, M., Bolker, B., Borcard, D., Carvalho, G., Chirico, M., De Caceres, M., Durand, S., Evangelista, H. B. A., FitzJohn, R., Friendly, M., Furneaux, B., Hannigan, G., Hill, M. O., Lahti, L., McGlinn, D., Ouellette, M.-H., Ribeiro Cunha, E., Smith, T., Stier, A., Ter Braak, C. J. F., and Weedon, J.: Vegan: Community ecology package, R package

https://doi.org/10.5194/egusphere-2025-3763
Preprint. Discussion started: 25 August 2025

version 2.6-8, https://CRAN.R-project.org/package=vegan, 2024.

Phillips, S. J., Anderson, R. P., and Schapire, R. E.: Maximum entropy modeling of species geographic distributions, Ecol. Model., 190, 231–259, https://doi.org/10.1016/j.ecolmodel.2005.03.026, 2006.

Qiu, B. and Imasato, N.: A numerical study on the formation of the Kuroshio Counter Current and the Kuroshio Branch Current in the East China Sea, Cont. Shelf Res., 10, 165–184, https://doi.org/10.1016/0278-4343(90)90028-K, 1990.

Reagan, J. R., Seidov, D., Wang, Z., Dukhovskoy, D., Boyer, T. P., Locarnini, R. A., Baranova, O. K., Mishonov, A. V., Garcia, H. E., Bouchard, C., Cross, S. L., and Paver, C. R.: World Ocean Atlas 2023, Volume 2: Salinity, https://doi.org /10.25923/70qt-9574, 2024.

Sargent, E. C., Hitchcock, A., Johansson, S. A., Langlois, R., Moore, C. M., LaRoche, J., Poulton, A. J., and Bibby, T. S.: Evidence for polyploidy in the globally important diazotroph *Trichodesmium*, FEMS Microbiol. Lett., 363, fnw244, https://doi.org/10.1093/femsle/fnw244, 2016.

Sato, T., Yamaguchi, T., Hidataka, K., Sogawa, S., Setou, T., Kodama, T., Shiozaki, T., and Takahashi, K.: Grazing mortality as a controlling factor in the uncultured non-cyanobacterial diazotroph (Gamma A) around the Kuroshio region, Biogeosciences, 22, 625–639, https://doi.org/10.5194/bg-22-625-2025, 2025.

Schvarcz, C. R., Wilson, S. T., Caffin, M., Stancheva, R., Li, Q., Turk-Kubo, K. A., White, A. E., Karl, D. M., Zehr, J. P., and Steward, G. F.: Overlooked and widespread pennate diatom-diazotroph symbioses in the sea, Nat. Commun., 13, 799, https://doi.org/10.1038/s41467-022-28065-6, 2022.

Shao, Z. and Luo, Y.-W.: Controlling factors on the global distribution of a representative marine non-cyanobacterial diazotroph phylotype (Gamma A), Biogeosciences, 19, 2939–2952, https://doi.org/10.5194/bg-19-2939-2022, 2022.

Shao, Z., Xu, Y., Wang, H., Luo, W., Wang, L., Huang, Y., Agawin, N. S. R., Ahmed, A., Benavides, M., Bentzon-Tilia, M., Berman-Frank, I., Berthelot, H., Biegala, I. C., Bif, M. B., Bode, A., Bonnet, S., Bronk, D. A., Brown, M. V., Campbell, L., Capone, D. G., Carpenter, E. J., Cassar, N., Chang, B. X., Chappell, D., Chen, Y. L., Church, M. J., Cornejo-Castillo, F. M., Detoni, A. M. S., Doney, S. C., Dupouy, C., Estrada, M., Fernandez, C., Fernández-Castro, B., Fonseca-Batista, D., Foster, R. A., Furuya, K.,

https://doi.org/10.5194/egusphere-2025-3763
Preprint. Discussion started: 25 August 2025

Garcia, N., Goto, K., Gago, J., Gradoville, M. R., Hamersley, M. R., Henke, B. A., Hörstmann, C., Jayakumar, A., Jiang, Z., Kao, S.-J., Karl, D. M., Kittu, L. R., Knapp, A. N., Kumar, S., LaRoche, J., Liu, H., Liu, J., Lory, C., Löscher, C. R., Marañón, E., Messer, L. F., Mills, M. M., Mohr, W., Moisander, P. H., Mahaffey, C., Moore, R., Mouriño-Carballido, B., Mulholland, M. R., Nakaoka, S., Needoba, J. A., Raes, E. J., Rahav, E., Ramírez-Cárdenas, T., Reeder, C. F., Riemann, L., Riou, V., Robidart, J. C., Sarma, V. V. S. S., Sato, T., Saxena, H., Selden, C., Seymour, J. R., Shi, D., Shiozaki, T., Singh, A., Sipler, R. E., Sun, J., Suzuki, K., Takahashi, K., Tan, Y., Tang, W., Tremblay, J.-É., Turk-Kubo, K., Wen, Z., White, A. E., Wilson, S. T., Yoshida, T., Zehr, J. P., Zhang, R., Zhang, Y., and Luo, Y.-W.: Global oceanic diazotroph database version 2 and elevated estimate of global oceanic N_2 fixation, Earth Syst. Sci. Data, 15, 3673–3709, https://doi.org/10.5194/essd-15-3673-2023, 2023.

Shen, H., Wan, X. S., Zou, W., Dai, M., Xu, M. N., and Kao, S.-J.: Light-driven integration of diazotroph-derived nitrogen in euphotic nitrogen cycle, Nat. Commun., 15, 9193, https://doi.org/10.1038/s41467-024-53067-x, 2024.

Shiozaki, T., Ijichi, M., Kodama, T., Takeda, S., and Furuya, K.: Heterotrophic bacteria as major nitrogen fixers in the euphotic zone of the Indian Ocean, Glob. Biogeochem. Cycles, 28, 1096–1110, https://doi.org/10.1002/2014GB004886, 2014.

Shiozaki, T., Takeda, S., Itoh, S., Kodama, T., Liu, X., Hashihama, F., and Furuya, K.: Why is *Trichodesmium* abundant in the Kuroshio? Biogeosciences, 12, 6931–6943, https://doi.org/10.5194/bg-12-6931-2015, 2015.

Shiozaki, T., Kondo, Y., Yuasa, D., and Takeda, S.: Distribution of major diazotrophs in the surface water of the Kuroshio from northeastern Taiwan to south of mainland Japan, J. Plankton Res., 40, 407–419, https://doi.org/10.1093/plankt/fby027, 2018.

Shrikumar, A., Lawrence, R., Casciotti, K. L: PYOMPA version 0.3: Technical note, ESS Open Archive [preprint], https://doi.org/10.1002/essoar.10507053.4, 04 February 2022.

Stenegren, M., Caputo, A., Berg, C., Bonnet, S., and Foster, R. A.: Distribution and drivers of symbiotic and free-living diazotrophic cyanobacteria in the western tropical South Pacific, Biogeosciences, 15, 1559–1578, https://doi.org/10.5194/bg-15-1559-2018, 2018.

https://doi.org/10.5194/egusphere-2025-3763
Preprint. Discussion started: 25 August 2025

Sun, J., Gu, X. Y., Feng, Y. Y., Jin, S. F., Jiang, W. S., Jin, H. Y., and Chen, J. F.: Summer and winter living coccolithophores in the Yellow Sea and the East China Sea, Biogeosciences, 11, 779–806, https://doi.org/10.5194/bg-11-779-2014, 2014.

Sun, Z., Zhu, Y., Jiang, Y., Zhai, H., Chen, J., Yan, X., Zeng, J., Chen, Q., and Jiang, Z.: Intrusion of Kuroshio enhances phytoplankton biomass and diversity in the East China Sea, J. Geophys. Res.-Ocean., 130, e2024JC021337, https://doi.org/10.1029/2024JC021337, 2025.

Tang, W. and Cassar, N.: Data-driven modeling of the distribution of diazotrophs in the global ocean, Geophys. Res. Lett., 46, 12258–12269, https://doi.org/10.1029/2019GL084376, 2019.

Tang, W., Wang, S., Fonseca-Batista, D., Dehairs, F., Gifford, S., Gonzalez, A. G., Gallinari, M., Planquette, H., Sarthou, G., and Cassar, N.: Revisiting the distribution of oceanic N_2 fixation and estimating diazotrophic contribution to marine production, Nat. Commun., 10, 831, https://doi.org/10.1038/s41467-019-08640-0, 2019.

Thompson, A., Carter, B. J., Turk-Kubo, K., Malfatti, F., Azam, F., and Zehr, J. P.: Genetic diversity of the unicellular nitrogen-fixing cyanobacteria UCYN-A and its prymnesiophyte host: UCYN-A genetic diversity, Environ. Microbiol., 16, 3238–3249, https://doi.org/10.1111/1462-2920.12490, 2014.

Tomczak, M. and Large, D. G. B.: Optimum multiparameter analysis of mixing in the thermocline of the eastern Indian Ocean, J. Geophys. Res.-Ocean., 94, 16141–16149, https://doi.org/10.1029/JC094iC11p16141, 1989.

Tuo, S., Chen, Y., and Chen, H.: Low nitrate availability promotes diatom diazotroph associations in the marginal seas of the western Pacific, Aquat. Microb. Ecol., 73, 135–150, https://doi.org/10.3354/ame01715, 2014.

Tuo, S.-H., Mulholland, M. R., Chen, Y.-L. L., Chappell, P. D., and Chen, H.-Y.: Patterns in *Rhizosolenia*- and *Guinardia*-associated *Richelia* abundances in the tropical marginal seas of the western North Pacific, J. Plankton Res., 43, 338–352, https://doi.org/10.1093/plankt/fbab022, 2021.

Turk-Kubo, K. A., Achilles, K. M., Serros, T. R. C., Ochiai, M., Montoya, J. P., and Zehr, J. P.: Nitrogenase (*nifH*) gene expression in diazotrophic cyanobacteria in the tropical North Atlantic in response to nutrient amendments, Front. Microbiol., 3, https://doi.org/10.3389/fmicb.2012.00386, 2012.

https://doi.org/10.5194/egusphere-2025-3763
Preprint. Discussion started: 25 August 2025

Turk-Kubo, K. A., Frank, I. E., Hogan, M. E., Desnues, A., Bonnet, S., and Zehr, J. P.: Diazotroph community succession during the VAHINE mesocosm experiment (New Caledonia lagoon), Biogeosciences, 12, 7435–7452, https://doi.org/10.5194/bg-12-7435-2015, 2015.

Turk-Kubo, K. A., Connell, P., Caron, D., Hogan, M. E., Farnelid, H. M., and Zehr, J. P.: In situ diazotroph population dynamics under different resource ratios in the North Pacific Subtropical Gyre, Front. Microbiol., 3, 386, https://doi.org/10.3389/fmicb.2018.01616, 2018.

Tyrrell, T.: Large-scale latitudinal distribution of *Trichodesmium* spp. in the Atlantic Ocean, J. Plankton Res., 25, 405–416, https://doi.org/10.1093/plankt/25.4.405, 2003.

Vélez-Belchí, P., Centurioni, L. R., Lee, D.-K., Jan, S., and Niiler, P. P.: Eddy induced Kuroshio intrusions onto the continental shelf of the East China Sea, J. Mar. Res., 71, 83–107, https://doi.org/10.1357/002224013807343470, 2013.

Wang, W.-L., Moore, J. K., Martiny, A. C., and Primeau, F. W.: Convergent estimates of marine nitrogen fixation, Nature, 566, 205–211, https://doi.org/10.1038/s41586-019-0911-2, 2019.

Wasimuddin, Schlaeppi, K., Ronchi, F., Leib, S. L., Erb, M., and Ramette, A.: Evaluation of primer pairs for microbiome profiling from soils to humans within the One Health framework, Mol. Ecol. Resour., 20, 1558–1571, https://doi.org/10.1111/1755-0998.13215, 2020.

Webb, E. A., Jakuba, R. W., Moffett, J. W., and Dyhrman, S. T.: Molecular assessment of phosphorus and iron physiology in *Trichodesmium* populations from the western Central and western South Atlantic, Limnol. Oceanogr., 52, 2221–2232, https://doi.org/10.4319/lo.2007.52.5.2221, 2007.

Webb, E. A., Ehrenreich, I. M., Brown, S. L., Valois, F. W., and Waterbury, J. B.: Phenotypic and genotypic characterization of multiple strains of the diazotrophic cyanobacterium, *Crocosphaera watsonii*, isolated from the open ocean, Environ. Microbiol., 11, 338–348, https://doi.org/10.1111/j.1462-2920.2008.01771.x, 2009.

Wen, Z., Browning, T. J., Cai, Y., Dai, R., Zhang, R., Du, C., Jiang, R., Lin, W., Liu, X., Cao, Z., Hong, H., Dai, M., and Shi, D.: Nutrient regulation of biological nitrogen fixation across the tropical western North Pacific, Sci. Adv., 8, eabl7564, https://doi.org/10.1126/sciadv.abl7564, 2022.

Wood, S. N.: Fast stable restricted maximum likelihood and marginal likelihood estimation of semiparametric

https://doi.org/10.5194/egusphere-2025-3763
Preprint. Discussion started: 25 August 2025

generalized linear models, J. R. Stat. Soc. B: Stat. Methodol., 73, 3–36, https://doi.org/10.1111/j.1467-9868.2010.00749.x, 2011.

Wu, C., Fu, F.-X., Sun, J., Thangaraj, S., and Pujari, L.: Nitrogen fixation by *Trichodesmium* and unicellular diazotrophs in the northern South China Sea and the Kuroshio in summer, Sci. Rep., 8, 2415, https://doi.org/10.1038/s41598-018-20743-0, 2018.

Xiao, W., Wang, L., Laws, E., Xie, Y., Chen, J., Liu, X., Chen, B., and Huang, B.: Realized niches explain spatial gradients in seasonal abundance of phytoplankton groups in the South China Sea, Prog. Oceanogr., 162, 223–239, https://doi.org/10.1016/j.pocean.2018.03.008, 2018.

Yang, D., Yin, B., Liu, Z., Bai, T., Qi, J., and Chen, H.: Numerical study on the pattern and origins of Kuroshio branches in the bottom water of southern East China Sea in summer, J. Geophys. Res.-Oceans, 117, 2011JC007528, https://doi.org/10.1029/2011JC007528, 2012.

Yang, D., Yin, B., Chai, F., Feng, X., Xue, H., Gao, G., and Yu, F.: The onshore intrusion of Kuroshio subsurface water from February to July and a mechanism for the intrusion variation, Prog. Oceanogr., 167, 97–115, https://doi.org/10.1016/j.pocean.2018.08.004, 2018.

Yang, H., Cai, J., Wu, L., Guo, H., Chen, Z., Jing, Z., and Gan, B.: The intensifying East China Sea Kuroshio and disappearing Ryukyu Current in a warming climate, Geophys. Res. Lett., 51, e2023GL106944, https://doi.org/10.1029/2023GL106944, 2024.

Yin, M., Li, X., Xiao, Z., and Li, C.: Relationships between intensity of the Kuroshio current in the East China Sea and the East Asian winter monsoon, Acta Oceanol. Sin., 37, 8–19, https://doi.org/10.1007/s13131-018-1240-2, 2018.

Yu, G.: Scatterpie: Scatter pie plot. R package version 0.2.5, https://CRAN.R-project.org/package=scatterpie, 2025.

Yue, J., Noman, M. A., and Sun, J.: Kuroshio intrusion drives the *Trichodesmium* assemblage and shapes the phytoplankton community during spring in the East China Sea, J. Oceanol. Limnol., 39, 536–549, https://doi.org/10.1007/s00343-020-9344-x, 2021.

Zehr, J. P. and Capone, D. G.: Changing perspectives in marine nitrogen fixation, Science, 368, eaay9514, https://doi.org/10.1126/science.aay9514, 2020.

https://doi.org/10.5194/egusphere-2025-3763
Preprint. Discussion started: 25 August 2025

Zehr, J. P., Bench, S. R., Mondragon, E. A., McCarren, J., and DeLong, E. F.: Low genomic diversity in tropical oceanic N_2-fixing cyanobacteria, Proc. Natl. Acad. Sci., 104, 17807–17812, https://doi.org/10.1073/pnas.0701017104, 2007.

Zhang, H., Mai, G., Luo, W., Chen, M., Duan, R., and Shi, T.: Changes in diazotrophic community structure associated with Kuroshio succession in the northern South China Sea, Biogeosciences, 21, 2529–2546, https://doi.org/10.5194/bg-21-2529-2024, 2024.

Zhang, L., Liu, Z., Zhang, J., Hong, G. H., Park, Y., and Zhang, H. F.: Reevaluation of mixing among multiple water masses in the shelf: An example from the East China Sea, Cont. Shelf Res., 27, 1969–1979, https://doi.org/10.1016/j.csr.2007.04.002, 2007.

Zhang, R., Zhang, D., Chen, M., Jiang, Z., Wang, C., Zheng, M., Qiu, Y., and Huang, J.: N_2 fixation rate and diazotroph community structure in the western tropical North Pacific Ocean, Acta Oceanol. Sin., 38, 26–34, https://doi.org/10.1007/s13131-019-1513-4, 2019.

Zhong, Y., Liu, X., Xiao, W., Laws, E. A., Chen, J., Wang, L., Liu, S., Zhang, F., and Huang, B.: Phytoplankton community patterns in the Taiwan Strait match the characteristics of their realized niches, Prog. Oceanogr., 186, 102366, https://doi.org/10.1016/j.pocean.2020.102366, 2020.

Zhou, F., Xue, H., Huang, D., Xuan, J., Ni, X., Xiu, P., and Hao, Q.: Cross-shelf exchange in the shelf of the East China Sea, J. Geophys. Res.-Oceans, 120, 1545–1572, https://doi.org/10.1002/2014JC010567, 2015.

https://doi.org/10.5194/egusphere-2025-3763
Preprint. Discussion started: 25 August 2025

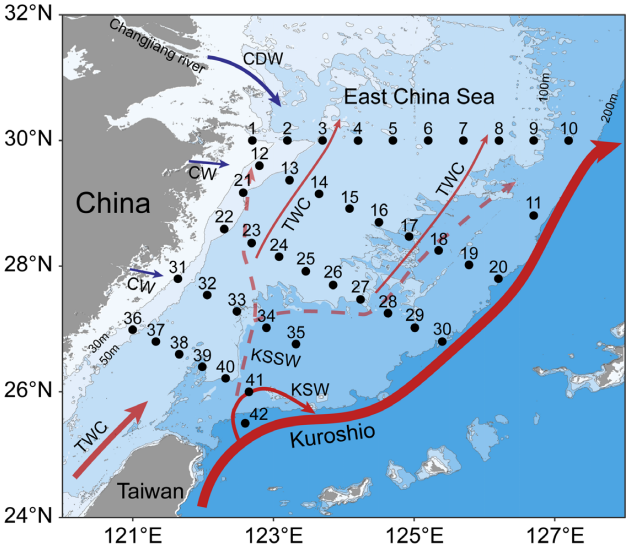

Figure 1. Sampling in the East China Sea (ECS) during the 2023 autumn and 2024 spring cruises. A total of 42 stations along 5 transects were selected for the collection of biological samples and environmental parameters. Transects A (stations 22–30) and B (stations 36–42) were chosen to investigate variations in biological and environmental factors along the vertical gradient extending from inshore to offshore. Major circulations are indicated, including the Changjiang diluted water (CDW), the Coastal water (CW), the Taiwan warm current (TWC), the Kuroshio current, the Kuroshio surface water (KSW) and the Kuroshio subsurface water (KSSW, dashed arrows) (Yang et al., 2012, 2018). Arrow sizes denote specific discharge rates (Liu et al., 2021). Land topography and ocean bathymetry data were obtained from the General Bathymetric Chart of the Oceans (GEBCO, https://www.gebco.net/, last access: 24 January 2025).

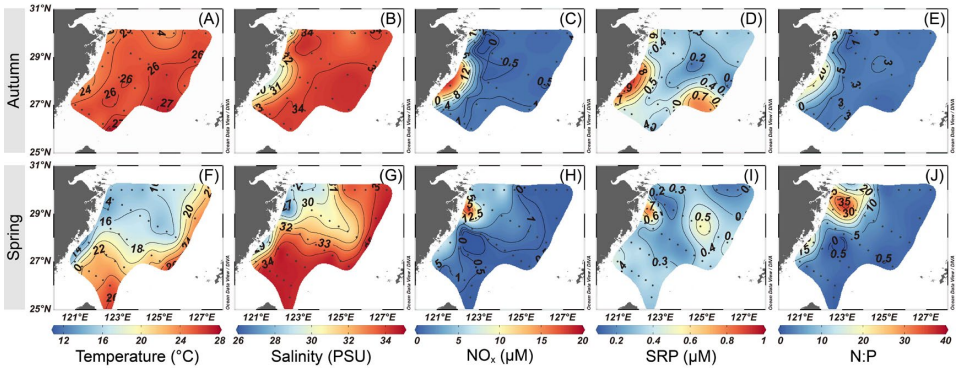

Figure 2. Variations in surface temperature (A, F), salinity (B, G), NO_x (C, H), SRP (D, I) and N:P ratio (E, J) during autumn (A–E) and spring (F–J) in the ECS. The map was created using Ocean Data View 5.7.2 (Schlitzer, Reiner, Ocean Data View, https://odv.awi.de, last access: 24 January 2025).

https://doi.org/10.5194/egusphere-2025-3763
Preprint. Discussion started: 25 August 2025

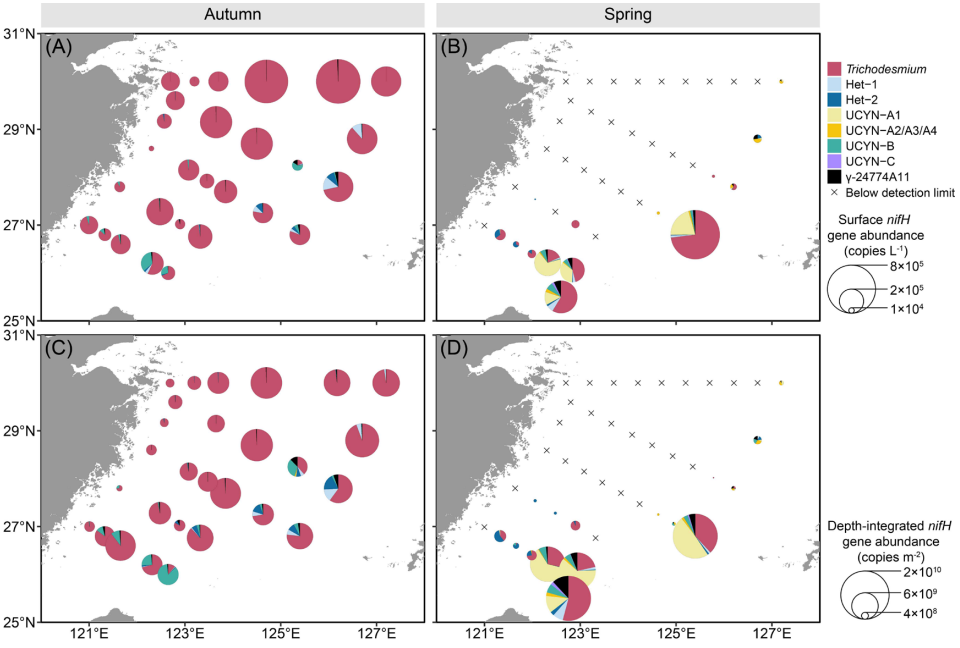

Figure 3. Surface (A, B) and depth-integrated (C, D) abundances of the eight major diazotrophic phylotypes in the ECS during autumn and spring as determined based on the quantification of the *nifH* gene (i.e., DNA-based) with TaqMan qPCR. Land topography was obtained from the General Bathymetric Chart of the Oceans (GEBCO, https://www.gebco.net/, last access: 24 January 2025).

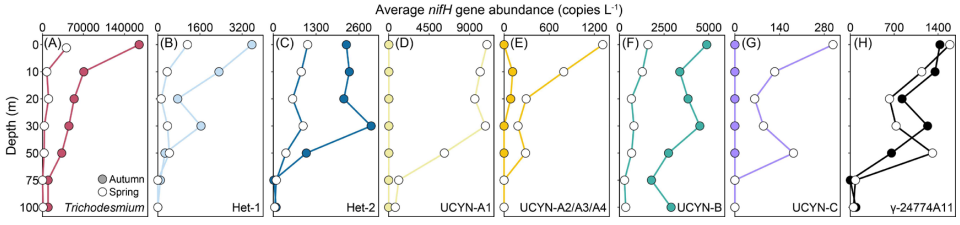

Figure 4. Vertical distributions in the abundances of the eight major diazotrophic phylotypes in the ECS during autumn and spring as determined based on the TaqMan qPCR assay of the *nifH* gene.

https://doi.org/10.5194/egusphere-2025-3763
Preprint. Discussion started: 25 August 2025

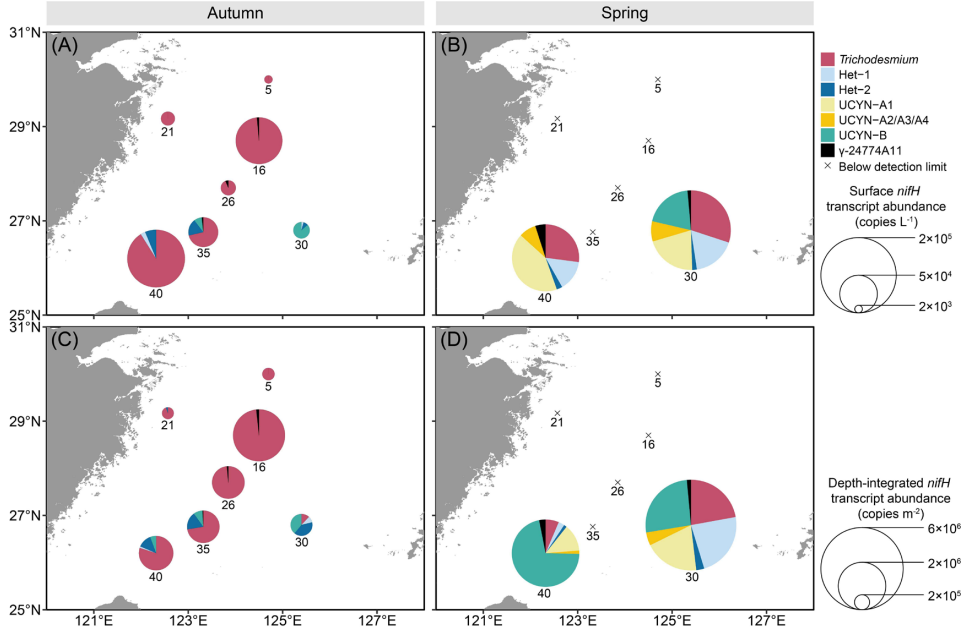

Figure 5. Surface (A, B) and depth-integrated (C, D) abundances of the seven major diazotrophic phylotypes in the ECS during autumn and spring as determined based on TaqMan qPCR assay of the *nifH* transcript (i.e., RNA-based). Note that the transcript abundance of UCYN-B was derived from nighttime samples, whereas that of the other groups was from daytime samples. The depth-integrated transcript abundance was calculated based on the integration of the upper 50 m of the water columns. Land topography was obtained from the General Bathymetric Chart of the Oceans (GEBCO, https://www.gebco.net/, last access: 24 January 2025).

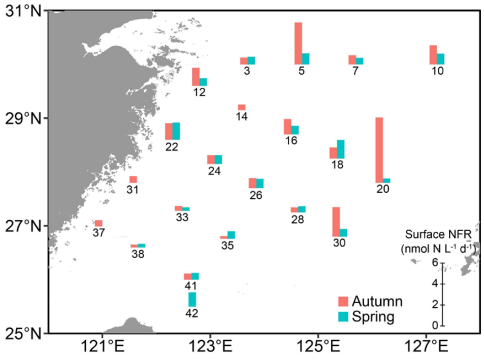

Figure 6. N_2 fixation rates in surface waters at designated stations in the ECS during autumn and spring as determined with in situ isotope tracing. Land topography was obtained from the General Bathymetric Chart of the Oceans (GEBCO, https://www.gebco.net/, last access: 24 January 2025).

https://doi.org/10.5194/egusphere-2025-3763
Preprint. Discussion started: 25 August 2025

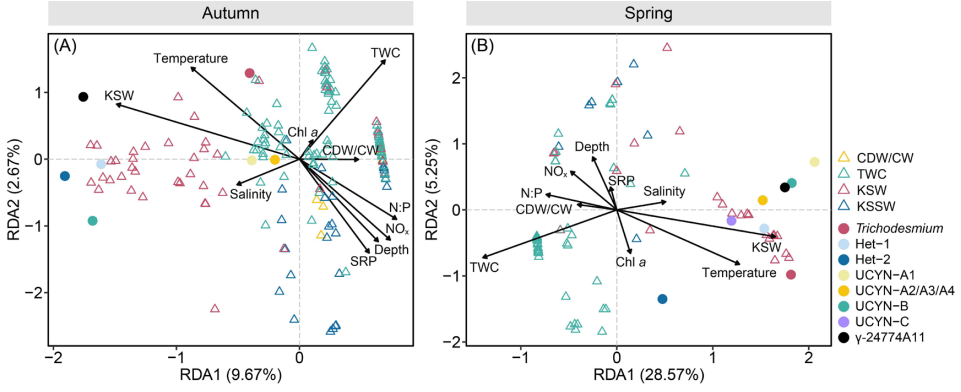

855

Figure 7. Correlation between diazotrophic phylotypes and environmental variables in distinct water masses in the ECS during autumn (A) and spring (B) as determined with redundancy analysis. Sampling stations are shown in triangles and color coded given the influence of different water masses. CDW, Changjiang diluted water; CW, Coastal water; TWC, Taiwan warm current; KSW, Kuroshio surface water; KSSW, Kuroshio subsurface water; Chl *a*, chlorophyll *a*.

860

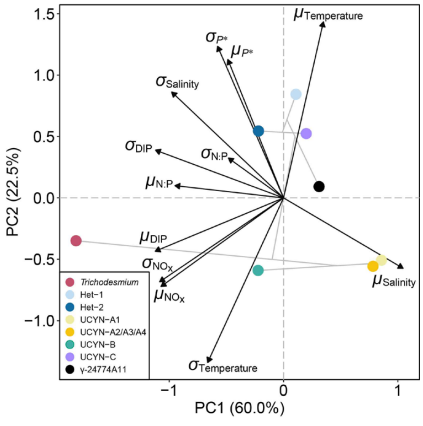

Figure 8. Principle component analysis depicting the ordination of niche mean (μ) and breadth (σ) corresponding to each individual environmental variable relative to each diazotrophic phylotype in the ECS. Clustering among the diazotrophs is shown in grey lines.